J Mol Model (2003) 9:164–171
DOI 10.1007/s00894-003-0128-y

ORIGINAL PAPER

Peter Carlqvist · Robert Eklund · Karl Hult · Tore Brinck

Rational design of a lipase to accommodate catalysis of Baeyer–Villiger oxidation with hydrogen peroxide

Received: 19 December 2002 / Accepted: 18 February 2003 / Published online: 17 April 2003

Abstract The mechanism and potential energy surface for the Baeyer–Villiger oxidation of acetone with hydrogen peroxide catalyzed by a Ser105–Ala mutant of *Candida antarctica* Lipase B has been determined using ab initio and density functional theories. Initial substrate binding has been studied using an automated docking procedure and molecular dynamics simulations. Substrates were found to bind to the active site of the mutant. The activation energy for the first step of the reaction, the nucleophilic attack of hydrogen peroxide on the carbonyl carbon of hydrogen peroxide, was calculated to be 4.4 kcal mol^{-1} at the B3LYP/6-31+G* level. The second step, involving the migration of the alkyl group, was found to be the rate-determining step with a computed activation energy of 19.9 kcal mol^{-1} relative the reactant complex. Both steps were found to be lowered considerably in the reaction catalyzed by the mutated lipase, compared to the uncatalyzed reaction. The first step was lowered by 36.0 kcal mol^{-1} and the second step by 19.5 kcal mol^{-1}. The second step of the reaction, the rearrangement step, has a high barrier of 27.7 kcal mol^{-1} relative to the Criegee intermediate. This could lead to an accumulation of the intermediate. It is not clear whether this result is an artifact of the computational procedure, or an indication that further mutations of the active site are required.

Keywords Density functional theory · *Candida antarctica* Lipase B · Rational design

P. Carlqvist · R. Eklund · T. Brinck (✉)
Physical Chemistry, Royal Institute of Technology,
100 44, Stockholm, Sweden
e-mail: tore@physchem.kth.se

K. Hult
Department of Biotechnology, Royal Institute of Technology,
AlbaNova, 106 91, Stockholm, Sweden

Present address:
R. Eklund, Organic Chemistry, Stockholm University,
106 91, Stockholm, Sweden

Introduction

The increased knowledge in structural biology and molecular enzymology opens the possibility to redesign not only substrate specificity, but also reaction specificity of enzymes. In this work we address the possibility of using a modified lipase to catalyze Baeyer–Villiger oxidation of acetone using hydrogen peroxide as oxidant. The specific enzyme we considered in our calculations is the lipase B from *Candida antarctica* (CALB). This lipase is a serine hydrolase and belongs to the group of α/β-hydrolases. The general features of the reaction center in CALB (Fig. 1) consist of the amino acid residues His224, Asp187, Ser105, Gln106, and Thr40. [1]

The histidine together with aspartate and the serine constitute the well-known catalytic triad. [1] The glutamine and threonine together form the oxyanion hole, which stabilizes the negative charge on the carbonyl oxygen in the transition state through hydrogen bonds. [1] It should be noted that threonine contributes with two hydrogen bonds to the oxyanion hole. Not only the NH group of the backbone, but also the OH group of the side-chain function as hydrogen bond donors. Site-directed mutagenesis experiments have shown that the hydrogen bond from the threonine OH group lowers the activation energy for ester hydrolysis by 3.5–4.5 kcal mol^{-1}. [2] In this work we have investigated the use of a Ser105–Ala mutation of CALB for catalysis of a Baeyer–Villiger oxidation. In a recent combined theoretical and experimental study, [3] such a mutated enzyme was shown to

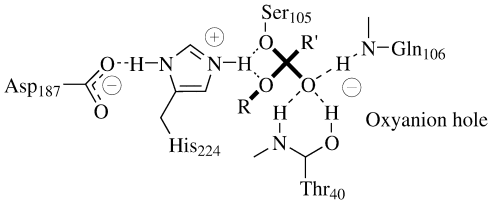

Fig. 1 *Candida antarctica* lipase B (CALB). The active site of the natural enzyme, with the transition structure of the substrate (*bold*)

catalyze aldol addition. Calculations showed favorable energetics for the addition reaction between two ketones or two aldehydes. Experiments performed with the enzyme and several aldehydes clearly showed an increased reaction rate when the aldol reaction was catalyzed by the mutant enzyme compared to the wild type lipase. Further experiments showed that the reaction actually takes place inside the active site of the enzyme. These results inspired us to investigate if the mutant could also be used as a catalyst for other carbonyl transformation reactions.

Baeyer–Villiger oxidation, which involves the transformation of ketones to esters and lactones, is one of the more important reactions in synthetic organic chemistry. The reaction is readily performed using peracids as the oxygen-donating reactant. [4, 5] Especially peracids with electron-withdrawing groups, such as trifluoroperacetic acid, are powerful reagents for this reaction. [4, 5, 6] In contrast, the use of simple peroxides requires addition of strong catalysts or promoters, such as boron trifluoride (BF_3), to produce reasonable yields. [7] A number of enzymes have been found to catalyze the Baeyer–Villiger reaction. [8, 9] For example, monooxygenases and dioxygenases incorporate one or two oxygen atoms from molecular oxygen (O_2), respectively, into the substrate. Most of these enzymes are dependent on NADPH or other cofactors for the catalytic process. Studies have shown that some lipases can catalyze Baeyer–Villiger oxidation from hydrogen peroxide without the need of any explicit cofactors. [10, 11] The mechanism for this process is not fully understood, and it has been argued that the enzymes only catalyze the formation of peracids and that the actual reaction takes place outside the enzyme. [11] In this project the objective has been to achieve a controlled catalytic reaction in the enzyme's active site with hydrogen peroxide functioning as the oxygen-donating reactant. The well-established catalytic effect of the catalytic triad together with the oxyanion hole and the fact that CALB is not dependent on any cofactors that need regeneration are the benefits of using CALB for this purpose. Two other advantages with the enzyme are that its activity remains high both in organic solvents and in moderate concentrations of hydrogen peroxide. [12] The main advantage of using an enzyme as a catalyst in organic reactions is that they can be performed stereoselectively.

To take advantage of CALB's catalytic ability and to ensure that the enzyme actually catalyzes the reaction, the enzyme must be modified by site-directed mutagenesis. In its natural form the reaction center's serine (Ser105) aided by the histidine (His224) acts as a nucleophile; the hydroxyl oxygen of the serine attacks the carbonyl carbon of the peptide/ester. Thus, to facilitate the attack of an external nucleophile, i.e. hydrogen peroxide, it is necessary to obstruct the function of Ser105. This can be achieved by a mutation of Ser105 for a nonpolar residue, such as alanine. After the mutation, the active site is devoid of its own nucleophile and the histidine can now aid the alternative nucleophile hydrogen peroxide. The

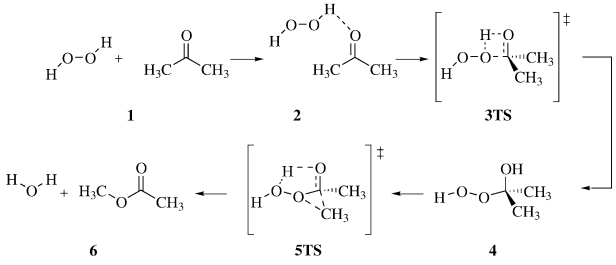

Scheme 1 Mechanism for the uncatalyzed Baeyer–Villiger oxidation of acetone by hydrogen peroxide

binding of acetone should be facilitated due to the natural ability of the enzyme to bind carbonyl compounds. It has been shown that the substrate binding in serine hydrolases generally does not depend on the catalytic triad residues. This has, for example, been demonstrated by systematic mutations of the active site residues in subtilisin. [13] Mutation of one or more of the triad residues did not result in a lowering of the Michaelis' constant. Furthermore, it was shown that residual catalytic activity was present after alanine mutation of the complete catalytic triad. This demonstrates the capacity of the oxyanion hole for stabilization of transition states with oxyanion character.

The mechanism for the Baeyer–Villiger oxidation involving a peracid as oxygen-donating agent is fairly well understood. [14, 15, 16, 17, 18] It has been shown that the carboxyl moiety of the peracid plays an active role in the proton transfer in the migration step. [15, 16, 18] A similar proton transfer mechanism cannot be obtained with simple peroxides, and this may be one reason for the lower reactivity of the latter in Baeyer–Villiger oxidation. In a recent study, we investigated the uncatalyzed and BF_3-promoted Baeyer–Villiger reactions of acetone and hydrogen peroxide using quantum chemical methods. [19] Since this study is expected to be relevant for an understanding of an enzyme-controlled reaction involving hydrogen peroxide, we will give a brief review of the results. The uncatalyzed reaction (Scheme 1) starts from the reactants acetone and hydrogen peroxide (**1**). One of the peroxide's equivalent hydrogens forms a hydrogen bond to the carbonyl oxygen of acetone (**2**). This increases the negative charge on the peroxide's oxygen, which becomes a more potent nucleophile. The peroxide attacks the carbonyl center of acetone (**3TS**) forming the Criegee intermediate (**4**). The reaction proceeds through a rearrangement of the intermediate by an alkyl migration (**5TS**). One of the carbon–carbon bonds in acetone is broken and the methyl group migrates to the hydrogen peroxide's oxygen atom bonded to the carbonyl carbon. At the same time a proton transfer from the carbonyl oxygen to the second peroxide oxygen atom occurs, creating a good leaving group in the form of water (**6**). In a previous study we showed that the free energy of activation in solution for the formation of the Criegee intermediate is 46 kcal mol^{-1} and the second transition state lies at 51 kcal mol^{-1} above the reactants (see

Table 1 Relative energies (kcal mol^{-1}) of the stationary points in the uncatalyzed Baeyer–Villiger reaction. All values are taken from [18]. The definitions for the energetics (with respect to the reactants **1**) are: ΔE, classical energy; $\Delta G^0_g=\Delta E(\text{G2MS})+\Delta\Delta G_g$; $\Delta G^0_{sol}=\Delta G^0_g+\Delta\Delta G(1\text{ atm}\rightarrow 1\text{ M})+\Delta\Delta G_{PCM}$. $\Delta\Delta G_g$ was calculated at 298 K and 1 atm, with the vibrational frequencies obtained at the B3LYP/6-31+G* level. $\Delta\Delta G(1\text{ atm}\rightarrow 1\text{ M})$ is the correction factor (1.89 kcal mol^{-1} per molecule) for changing the standard state from 1 atm (0.041 M) to 1 M. The ΔG^0_{sol} values correspond to a standard state of 1 M solution in a solvent which has the same properties as pure acetone

	ΔE B3LYP/6-31+G*	ΔE MP2/6-31+G**	ΔE G2MS[a]	ΔG^0_g	ΔG^0_{sol}
1	0.0	0.0	0.0	0.0	0.0
2	−8.2	−9.0	−8.5	−1.4	1.0
3TS	32.2	32.8	32.7	42.3	45.6
4	−9.2	−15.5	−15.2	−0.4	2.3
5TS	38.0	42.1	38.0	48.9	51.3
6	−68.5	−73.8	−72.2	−70.9	−71.7

[a] G2MS (ΔE)=ΔE[MP2/6-311+G(2df.2p)]−$\triangle E$[MP2/6-31G*]+ΔE[CCSD(T)/6-31G*]

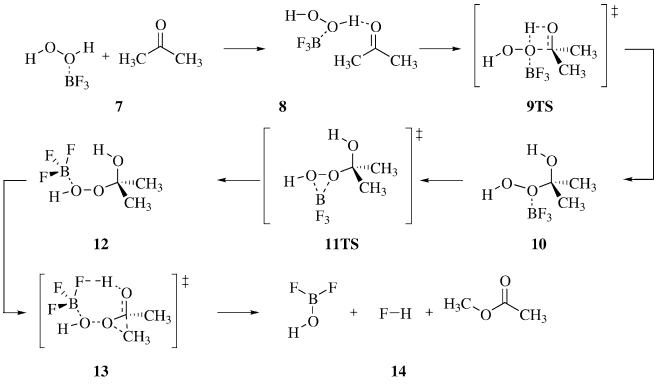

Scheme 2 Mechanism for the BF_3-promoted Baeyer–Villiger oxidation of acetone by hydrogen peroxide

Table 1). The results from that study showed that the uncatalyzed reaction, both in the gas phase and in solution, is so slow that essentially no observable product can be expected. In the same work we investigated the Baeyer–Villiger oxidation promoted by BF_3 (Scheme 2). It was found that BF_3 considerably lowered the free energies of the transition states energies to 16.2 kcal mol^{-1} for the formation of the Criegee intermediate and to 17.7 kcal mol^{-1} for the alkyl migration (Table 2). The initial step of the BF_3-promoted reaction is the formation of an H_2O_2–BF_3 complex (**7**). The electron-withdrawing capacity of BF_3 sufficiently weakens the O–H bond in hydrogen peroxide, which leads to a complete transfer of the hydrogen to the carbonyl oxygen of acetone in the transition step (**9TS**), whereas in the uncatalyzed reaction the proton is only partly transferred. Due to the same effect, the acidity of this group will also be increased, which results in a lower activation energy in the rearrangement step (**13TS**). Another interesting fact in the BF_3-promoted reaction is that the BF_3 is bound to the inner oxygen in the Criegee intermediate formed in the first step (**10**), but in the last reaction step, the migration of the alkyl group, BF_3 is bonded to the outer oxygen. The BF_3 transfers from the inner oxygen of the bound hydrogen peroxide to the outer via a new transition state (**11TS**) forming a second Criegee intermediate (**12**). In the migration step, the boron trifluoride forms BF_3OH as a leaving group, creating hydrogen fluoride and ester as products (**14**). The reaction mechanism for mainly the BF_3-promoted Baeyer–Villiger reaction was used as a starting point for the studies of the enzyme-catalyzed mechanism.

The objective of the current work has been to analyze the potential of the Ser105–Ala mutant of CALB for catalyzing the Baeyer–Villiger reaction by studying the full catalytic process. The initial binding of the substrate molecules has been studied using an automated docking procedure and by molecular dynamics (MD) simulations. The MD simulations provide information on free energies

Table 2 Relative energies (kcal mol^{-1}) of the stationary points in the BF_3-assisted Baeyer–Villiger reaction. All values are taken from [18]. The definitions for the energetics (with respect to the reactants **1**) are: ΔE, classical energy; $\Delta G^0_g=\Delta E(\text{MP2})+\Delta\Delta G_g$; $\Delta G^0_{sol}=\Delta G^0_g+\Delta\Delta G(1\text{ atm}\rightarrow 1\text{ M})+\Delta\Delta G_{PCM}$. $\Delta\Delta G_g$ was calculated at 298 K and 1 atm, with the vibrational frequencies obtained at the B3LYP/6-31+G* level. $\Delta\Delta G(1\text{ atm}\rightarrow 1\text{ M})$ is the correction factor (1.89 kcal mol^{-1} per molecule)for changing the standard state from 1 atm (0.041 M) to 1 M. The ΔG^0_{sol} values correspond to a standard state of 1 M solution in a solvent that has the same properties as pure acetone

	ΔE B3LYP/6-31+G*	ΔE MP2/6-31+G**	ΔG^0_g	ΔG^0_{sol}
7	0.0	0.0	0.0	0.0
8	−14.5	−17.6	−6.4	−2.6
9TS	10.8	9.8	23.2	16.2
10	−7.0	−16.6	−1.5	3.1
11TS	−4.5	−11.4	0.8	6.7
12	−9.0	−16.3	−0.9	0.7
13TS	7.5	6.3	20.4	17.7
14	−58.4	−63.7	−74.2	−70.8

of binding and the ability of the substrate molecules to maintain near-attack complexes that are productive for the catalytic process. In addition, structural changes induced by the mutation will be reflected in the structures obtained from the MD simulation. The actual catalytic reaction in the mutated enzyme has been studied by quantum chemical calculations. In a previous study we analyzed a natural reaction of serine hydrolase, the hydrolysis of esters. [20] It was shown that considerable information about the catalytic properties of the enzyme could be obtained from quantum chemical calculations on a rather limited model system. The model system consisted of methyl acetate, formate anion, imidazole, methanol and two water molecules, which represented the substrate, the catalytic triad (Asp–His–Ser) and the two oxyanion hydrogen bonds, respectively. Using this limited model we were able to study the full catalytic reaction. The calculated rate activation barriers for the acylation and deacylation steps were in good agreement with experimental studies of reaction rates. In addition, we were able to reproduce the observed effects on reaction rates from site-directed mutagenesis experiments of serine hydrolases by performing the calculations with and without the formate anion and the water molecules. On the basis of these results we decided to use a similar model in the current study. However, methanol was removed from the model to simulate the Ser105–Ala mutation, and three water molecules were included instead of two to give a better representation of the hydrogen bond network in the oxyanion hole of CALB. The positions of the water molecules relative the imidazole were estimated by a comparison with representative structures from an MD simulation on the mutated enzyme with a Criegee intermediate bound to the active site, and limited constraints were used in the quantum chemical calculation to preserve this positioning.

Methods and procedure

Docking

Binding of the substrate molecules acetone and hydrogen peroxide to the mutant enzyme was investigated initially using the Autodock 3.0 program package. [21] This program utilizes a Lamarckian genetic algorithm for the automated docking. During the simulation the interaction energy between ligand and the protein is evaluated using grid-based atomic affinity potentials. The final free energy of interaction is calculated with a free-energy-based expression that includes terms for the dispersion and repulsion energies, directional hydrogen bonding, screened electrostatics and desolvation. The force field has been calibrated to reproduce experimental binding energies for a set of 30 chemically diverse protein–ligand complexes. The protein structure for the docking studies was the CALB with HEE (*N*-hexylphosphonate ethyl ester) and NAG (*N*-acetyl-D-glucosamine) by Uppenberg et al. [1, Protein Data Bank entry 1LBS] The inhibitor, HEE, NAG and all the crystal waters were removed from the structure. The Ser105 was mutated to an alanine using the SwissPDBviewer program. [22] Simulations were performed with Asp134 both protonated and unprotonated. Charges for the protein atoms were taken from the original Amber united atom force field [23] as recommended in the Autodock manual. The substrate molecules were also treated using the united atom approach, and the charges were fitted to reproduce the ab initio HF/6-31G* electrostatic potential using the procedure of Merz et al. [24] The grid was of the size 60×60×60, with a spacing of 0.375 Å and was centered on the NE nitrogen of the catalytic residue His224. A total of 50 runs using the Lamarckian genetic algorithm were performed in each separate case. During the simulations, free rotation around carbon–carbon single bonds in the substrate molecules was allowed.

Molecular dynamics

Selected docked structures were used in subsequent MD simulations with the purpose of estimating binding energies and studying the dynamic properties of possible near-attack complexes. The method used to calculate the free energy of binding is a semiempirical approach called the linear interaction energy (LIE) method. [25, 26] It is similar to the free energy perturbation (FEP) method [27] in that both are based on the use of thermodynamic cycles, but the LIE method is not as computationally demanding. Whereas FEP demands a large number of simulations, the LIE method only requires two, one on the bound state and one on the free solvated state of the ligand. The method is based on considering the polar and nonpolar contributions to the total binding energy separately. The polar part is treated using the electrostatic linear response approximation while nonpolar interactions are treated using an empirical formula calibrated from a set of experimental data. The combination of these two approaches results in the following equation for the total binding energy:

$$\Delta G_{\text{bind}} = \alpha\{\langle V_{\text{l-s}}^{\text{vdw}}\rangle_{\text{bound}} - \langle V_{\text{l-s}}^{\text{vdw}}\rangle_{\text{free}}\} + \beta\{\langle V_{\text{l-s}}^{\text{el}}\rangle_{\text{bound}} - \langle V_{\text{l-s}}^{\text{el}}\rangle_{\text{free}}\} \quad (1)$$

The second part of Eq. (1) is derived from the linear response approximation and concerns the polar (electrostatic) contribution to the binding energy. The first part concerns the nonpolar contribution; these terms are given by the Lennard-Jones potential. The parameter α has been calibrated against experimental data for enzyme inhibition and has a value of 0.16. [26] According to the linear response approximation the value of β should be 0.5. [25] However, an analysis based on comparisons with FEP simulations has shown that this value is only appropriate for ionic compounds. [26] The value that should be used for a neutral substrate without hydroxyl groups, such as acetone, has been shown to be 0.43. [26] The terms of the equation are collected from sampling of two molecular dynamics simulations, one for the free state and one for the bound state.

MD simulations were carried out on spheres with the radius of 16 Å using a modified version [25, 26] of the GROMOS 87 [28] force field. The program Q was used for all MD calculations. [29] Parameters for the substrates were assigned in analogy with the amino acid residue parameters of the force field. In the simulation of the free state 615 SPC water molecules surrounded the substrate, giving a total number of 619 particles. The substrate was held in the center of the sphere by harmonic positional restraints. The bound state was composed of 3,241 particles with 141 SPC water molecules filling the sphere, which was centered on the active site. A total of 1,873 protein atoms were outside the sphere and were held fixed during the simulation. In the bound-state simulations only Asp187 was charged. An analysis of the hydrogen-bonding pattern in the crystal structure indicated that Asp134 and Glu188 should be protonated. Charged amino acid residues near the boundary of the sphere and those outside the sphere were treated using the neutral dipolar version of the GROMOS force field. [30]

The following protocol was used for the MD simulations: For the bound states, five warm-up steps precede the simulations. The warm-up steps are 4 ps each with a time step of 1 fs. In the first four steps the protein atoms and the substrate are restrained to their initial coordinates by a 5 kcal (mol Å^2)$^{-1}$ harmonic potential. All atoms in the sphere are free to move in the last warm-up run. The temperature is held constant during the simulations by coupling to a temperature bath. The first run is at 1 K, with a coupling constant of

1; the low coupling constant makes this simulation much like an energy minimization. The second run has a temperature of 50 K with a coupling constant of 5. The third run is at temperature 150 K, and the last two are at 300 K, all three with a bath coupling constant of 5. No energy data were sampled from the equilibration phase of the simulations. For the actual dynamics simulation and data acquisition, five 50-ps runs are performed, a total of 250 ps, at 300 K, a bath coupling constant of 10 and with a time step of 1 fs. For the simulations of the free state no warm-up runs are performed. Five simulations at a temperature of 300 K and a bath coupling constant of 10 are performed. The carbonyl carbon of the substrate is restrained with harmonic positional restraints (50 kcal (mol Å^2)$^{-1}$).

Quantum chemical calculations

Geometries of the stationary points (minima and transition states) involved in the reaction were fully optimized at the B3LYP/6-31G level, using extra basis functions on chemically important atoms; diffuse functions were added to the heavy atoms in the substrate, to the oxygens in hydrogen peroxide and to the two formate oxygens; *d*-functions were added to the same atoms mentioned above and to the two nitrogens of imidazole. As already mentioned, the positions of the water molecules representing the oxyanion hole were submitted to geometrical constraint based on a structure from an MD simulation on the Ser105–Ala mutant with the Criegee intermediate bound to the active site. In particular, the positioning of the water molecules relative each other was constrained, and also the angular positioning of the water molecules relative to the histidine. However, the distance between the water molecule cluster and the histidine was allowed to vary. Single point energies were calculated at the B3LYP/6-31G (extra basis) optimized geometries using B3LYP/6-31+G*. Since there have been indications that the combination of Becke's [31] three-parameter mixing of exchange (B3) and the Lee–Young–Parr [32] correlation (LYP) functional underestimates the barriers of certain reactions, such as open shell and proton transfer reactions, [33, 34] we also calculated the energies using MP2/6-31+G*. It is generally considered that MP2 produces relative energies for closed shell systems of similar accuracy to B3LYP. The use of geometrical constraints prevented the calculation of vibrational frequencies. Thus, no energy correction terms due to zero-point or thermal motion have been incorporated in the results. The Gaussian 98 [35] suite of programs was used for all quantum chemical calculations.

Results and discussion

Substrate binding

The binding of three potential carbonyl substrates, acetone, propanal and 3-pentanone was investigated using both the automated docking procedure and molecular dynamics simulations. In all docking calculations the oxyanion hole was identified as the most favorable binding site, despite the fact that several different starting coordinates were tested for the substrate molecules. In addition, 80–98% of the simulation runs in each calculation found the oxyanion hole as the binding site. The calculated binding energies are listed in Table 3. Acetone and propanal have similar binding free energies, 3.05 kcal mol^{-1} and 3.51 kcal mol^{-1}, respectively, while the binding energy of 3-pentanone is more than 1 kcal mol^{-1} lower. The binding energies obtained from the MD simulations using the LIE approach show similar differences between the substrates, but indicate a significantly weaker substrate binding.

Table 3 Computed free energies of substrate binding to the Ser105–Ala mutant of CALB, all energies in kcal mol^{-1}

	ΔG^0_{bind} [a]	ΔG^0_{bind} [b]
Acetone	–3.05	–0.09
Propanal	–3.51	–0.48
3-Pentanone	–4.54	–1.80

[a] Computed using Autodock, see Methods and procedure for details
[b] Computed using the LIE method, see Methods and procedure for details

An analysis of the different energy components from the LIE calculations does not provide a clear answer to the origin of the observed binding energy differences. However, these data, together with trajectory information from the MD simulations, indicate that the increasing hydrophobicity with chain length is the most reasonable explanation. During the MD simulations, 3-pentanone stayed tightly bound to the oxyanion hole, while acetone tended to leave occasionally and form hydrogen bonds to the solvent instead. It is clear that the substrate binding will be heavily influenced by the choice of solvent. In particular for the shorter carbonyl compounds, it can be expected that the use of aprotic and nonpolar solvents will increase the binding affinity. We also investigated the binding of hydrogen peroxide to the active site using Autodock and MD simulations. In these cases we had the oxyanion hole already occupied by an acetone molecule. The Autodock simulations showed that there are a large number of binding sites for hydrogen peroxide in the vicinity of the active site. Binding of the peroxide to the NE nitrogen of HIS 224 is not one of the most preferred, since this binding configuration only involves forming one hydrogen bond with the enzyme. MD simulations starting from this configuration showed that the peroxide was not tightly bound to the histidine. The conclusions that can be made from these results are that the hydrogen peroxide concentration must be rather high and that a rather nonpolar solvent must be used in order to ensure that a stable hydrogen bond is formed between the peroxide and HIS 224, and consequently, the peroxide is kept in a favorable near-attack complex.

Reaction mechanism

The enzyme-catalyzed reaction mechanism (Scheme 3 and Table 4) seems to resemble the BF_3-promoted reaction (Scheme 2). In the first structure (**15**) the acetone is hydrogen bonded to the oxyanion hole and the hydrogen peroxide acts like Ser105 in the natural enzyme, i.e. it is hydrogen bonded to the histidine. This is essentially what is called the near-attack complex of the enzymatic reaction. Compared to the uncatalyzed and BF_3-promoted reactions, this structure most closely resembles the initial complexes, **1** and **8**, respectively, and when comparing these two reactions we will discuss

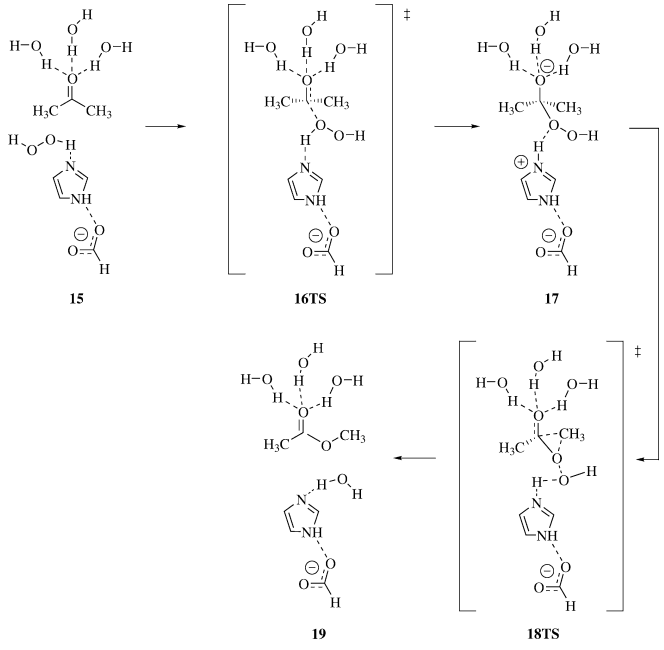

Scheme 3 Mechanism for the enzyme-catalyzed Baeyer–Villiger oxidation of acetone by hydrogen peroxide

Table 4 Relative energies (kcal mol^{-1}) of the stationary points in the Baeyer–Villiger reaction catalyzed by Ser–Ala CALB mutant. The energies presented are single point calculations on the optimized geometries. The optimizations were done using B3LYP/6-31G with extra basis functions on chemically important atoms, see Methods and procedure for details

	ΔE B3LYP/6-31+G*	ΔE MP2/6-31+G*
15	0.0	0.0
16TS	4.4	2.8
17	−7.8	−12.9
18TS	19.9	19.6
19	−68.0	−73.7

the energetics relative the initial complexes. In these comparisons we do not initially take into account the effects of vibrational corrections and solvation effects on the energetics. Unless otherwise specified the energetic data are computed at the B3LYP/6-31+G* level.

The first transition step of the reaction (**16TS**) is stabilized by a number of interactions (see Fig. 2). The build up of negative charge on the carbonyl oxygen of acetone is stabilized by the oxyanion hole through hydrogen bonds. The histidine accepts the proton from hydrogen peroxide, and the positive charge that appears is stabilized by the negative aspartate. The enzyme effectively stabilizes the charge separation in the transition state, thus lowering the activation energy. The energy for the transition state is only 4.4 kcal mol^{-1} above the initial complex, which indicates that this first step is very well catalyzed by the enzyme. This is further emphasized by the fact that this step in the uncatalyzed reaction has an activation energy of more than 40 kcal mol^{-1}. Also the

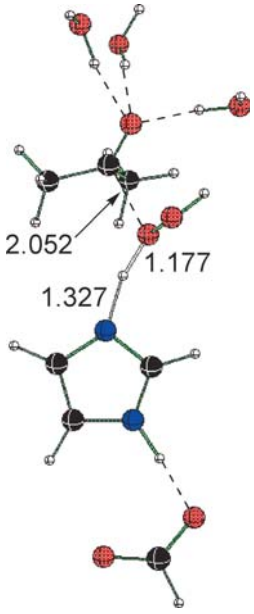

Fig. 2 First TS (**16TS**) in the Baeyer–Villiger oxidation in a mutant of CALB. Distances in Å

BF_3-promoted reaction has a relatively high activation energy, 25.3 kcal mol^{-1}.

The Criegee intermediate (**17**) formed in the first step of the reaction is more stable relative the reactant complex than its counterpart in the BF_3-promoted reaction, −7.8 kcal mol^{-1} compared to +7.5 kcal mol^{-1} at the B3LYP/6-31+G* level of theory. It is also more stable than the Criegee intermediate of the uncatalyzed reaction, which is 1.0 kcal mol^{-1} above the initial complex. It is not surprising that the enzyme is able to stabilize an oxyanion intermediate strongly, since the serine hydrolases are optimized by nature for this task. The stabilization is largely electrostatic in nature and has two major components, the hydrogen bonding to the oxyanion in the oxyanion hole and the stabilization of the protonated histidine by the hydrogen bonding to the negative Asp187.

In our previous work where we studied the BF_3-promoted Baeyer–Villiger reaction, we found that the reaction proceeds via two Criegee intermediates. In the first, BF_3 is bonded to the "inner" oxygen of hydrogen peroxide, i.e. the oxygen that attacks the carbonyl center. The BF_3 is then transferred to the outer oxygen in order to promote the rearrangement step of the reaction. The transition state for the BF_3 transfer was found to have an activation energy of 2.5 kcal mol^{-1} relative the first Criegee intermediate. For the enzyme reaction we were not able to find a corresponding transition state and intermediate. Instead our calculations suggest that the transfer of the hydrogen bond from the inner to the outer oxygen and the rearrangement occur in a concerted fashion.

The last step of the reaction, the rearrangement step, proceeds via the transition state, **18TS**, and results in the formation of water and ester (see Fig. 3). The activation energy is 19.9 kcal mol^{-1} relative to the initial complex.

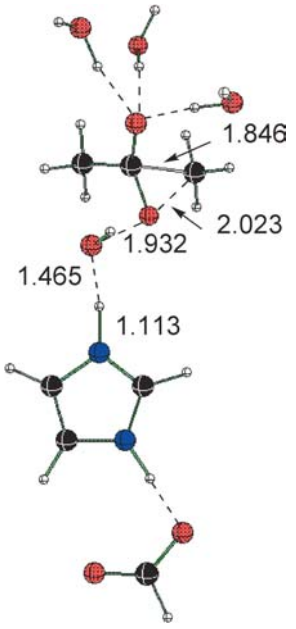

Fig. 3 Second TS (**18TS**) in the Baeyer–Villiger oxidation in a mutant of CALB. Distances in Å

Compared to the Criegee intermediate, **18TS** is even higher in energy, 27.7 kcal mol^{-1}. It should be noted that, even though the activation energy for the rearrangement step is relatively high, there is a considerable catalytic effect compared to the uncatalyzed reaction. In the uncatalyzed reaction the rearrangement transition state is 47 kcal mol^{-1} higher in energy than the Criegee intermediate. On the other hand, the catalytic effect of the enzyme is considerably smaller than for the BF_3-promoted reaction where the rearrangement transition state is only 16.5 kcal mol^{-1} above the second Criegee intermediate. For all three reactions, we note that the MP2 method predicts greater differences in energy than B3LYP between the Criegee intermediate and the rearrangement transition states. The results from the more accurate G2MS calculations on the uncatalyzed reaction indicates that the truth is probably somewhere in between the B3LYP and MP2 results.

Our calculations show that the rate-determining step of the Baeyer–Villiger reaction in the enzyme is the rearrangement step. This is in agreement with most catalyzed Baeyer–Villiger reactions in organic solutions. We also find that the enzyme has a considerable catalytic effect compared to the uncatalyzed reaction. The overall activation energy is lowered by more than 25 kcal mol^{-1} in the enzyme. However, the calculations indicate that the energy difference between the Criegee intermediate and the rearrangement transition state may be too high for effective catalysis. There is a considerable risk that the catalytic reaction will be halted due to an accumulation of Criegee intermediates in the enzyme molecules. The reason for the large energy gap between the transition state and the Criegee intermediate seems to be due to a too effective stabilization of the intermediate rather than a lack of transition state stabilization. In this context is important to try to understand if the overstabilization of the Criegee intermediate is real or an artifact of the limitations of our computational approach. It is obvious that we have used a rather limited model for the enzyme and that we have not considered the vibrational effects on the potential energy surface. Regarding, the vibrational motions it is well known that consideration of zero-point effects usually lowers activation barriers. For example, zero-point vibrations lower the energy difference between the last Criegee intermediate and the transition state for BF_3-promoted reaction by 1.7 kcal mol^{-1}. A similar reduction can probably be expected for the enzyme-catalyzed reaction. The entropy effects on the energy surface due to vibrational motions are harder to predict, but we can speculate that the transition state is about as rigid as the intermediate and consequently that the entropy effects are similar. This is also the case in the BF_3-promoted reaction.

Another effect that must be considered is the effect of the solvation from the enzyme environment on the potential energy surface of the reaction. Since our enzyme model is rather small, it can be expected that solvation effects are not fully accounted for. In the BF_3-promoted reaction the solvation effects from acetone, which we calculated by the PCM method, are rather important. The energy of the rearrangement transition state is lowered by 4.3 kcal mol^{-1} relative to the second Criegee intermediate. A similar effect is not unlikely for the enzyme-catalyzed reaction. It should also be noted that the constraints imposed in the calculations might lead to an unphysical stabilization of the Criegee intermediate relative the transition state. The frozen positions of the oxyanion water molecules were based on an MD simulation of the enzyme with a Criegee intermediate in the active site, and the Criegee intermediate is just one point on the potential energy surface and the hydrogen bond pattern may be different at other points. Thus, it can be expected that this structure does not provide an optimal position of the oxyanion hole relative the histidine for the rearrangement transition state. We do not expect this effect to be large, but it may amount to a 5–6-kcal mol^{-1} destabilization of the transition state. However, the three effects together, i.e. the vibrational, solvation and constraints effects, could quite readily amount to an 8–9-kcal mol^{-1} lowering of the activation energy.

A further effect that should be considered when judging the catalytic ability of the modified enzyme is the fact that methyl is a very poor migratory group. One way to increase the reaction rate would be to use an unsymmetrical ketone with a better-suited migratory group such as *t*-butyl or a phenyl group with an electron-donating substituent.

Summary and conclusions

Docking simulations and MD simulations have shown the preference of the substrate to bind to the oxyanion hole. Evaluation of binding energies calculated through the LIE

method of three different substrates (acetone, propanal and 3-pentanone) did not give a clear picture of the binding preference of the substrates. However, the result indicate that the binding increases with increasing hydrophobicity, as it was found that 3-pentanone had the highest binding energy and stayed tightly bound to the oxyanion hole during the MD simulations.

For the first step of the Baeyer–Villiger oxidation, which is a nucleophilic attack by the hydrogen peroxide on the carbonyl carbon concomitant with a proton transfer from the peroxide to His224, the activation energy was calculated to be 4.4 kcal mol^{-1} and 2.8 kcal mol^{-1} at the B3LYP/6-31+G* and MP2/6-31+G* levels, respectively. Compared to the uncatalyzed reaction the activation energy is lowered by 36.0 kcal mol^{-1} (B3LYP/6-31+G*). This considerable reduction is due to the stabilizing effect of the oxyanion hole and Asp187. Together they stabilize the charge separation in the transition state through electrostatic interaction. The rate-determining step was found to be the rearrangement step, which is the second step of the reaction. This reaction step proceeds via a proton transfer, where the proton is transferred back to the peroxyl moiety bonded to acetone, thereby creating a good leaving group, water. Concerted with the proton transfer, the methyl group migrates to the oxygen bonded to the carbonyl carbon, and the product is formed. The activation energy for the rate-determining step was found to be 19.9 kcal mol^{-1} and 19.6 kcal mol^{-1} at the B3LYP/6-31+G* and MP2/6-31+G* levels, respectively, relative the reaction complex. This is a decrease in activation energy of 19.5 kcal mol^{-1} (B3LYP/6-31+G*) compared to the uncatalyzed reaction.

Although the activation energy for both steps in the reaction is lowered considerable compared to the uncatalyzed reaction, the second step barrier remains high. The activation energy for the rate-determining step is 27.6 kcal mol^{-1} at the B3LYP/6-31+G* level, and 32.6 kcal mol^{-1} at the MP2/6-31+G* level, relative the Criegee intermediate. This high energy barrier could lead to an accumulation of the intermediate in the enzyme molecules. It is not clear whether this result is an artifact of the computational procedure, or if it should be taken as an indication that further mutations of the active site are required for effective catalysis. The results together with those of a previous study [3] show that CALB with suitable mutations has the potential to catalyze a wide range of carbonyl transformations, including the Baeyer–Villiger oxidation.

Acknowledgement This work was supported by computing resources by the Swedish National Allocations Committee (SNAC).

References

1. Uppenberg J, Ohrner N, Norin M, Hult K, Kleywegt GJ, Patkar S, Waagen V, Anthonsen T, Jones TA (1995) Biochemistry 34:16838–16851
2. Magnusson A, Hult K, Holmquist M (2001) J Am Chem Soc 123:4354–4355
3. Branneby C, Carlqvist P, Magnusson A, Hult K, Brinck T, Berglund P (2003) J Am Chem Soc 125:874–875
4. Plesnicar B (1983) In: Patai S (ed) The chemistry of peroxides. Wiley, Chichester, p 559 and references therein
5. Renz M, Meunier B (1999) Eur J Org Chem 4:737–750 and references therein
6. Emmons WD, Lucas GB (1955) J Am Chem Soc 77:2287–2288
7. McClure J, Williams PH (1962) J Org Chem 27:24–26
8. Walsh CT, Chen YCJ (1988) Angew Chem Int Ed Engl 27:333–343 and references therein
9. Roberts SM, Wan PWH (1998) J Mol Catal B 4:111–136 and references therein
10. Lemoult SC, Richardson PF, Roberts SM (1995) J Chem Soc Perkin Trans 1 2:89–91
11. Pchelka BK, Gelo-Pujic M, Guibé-Jampel EJ (1998) J Chem Soc Perkin Trans 1 17:2625–2627
12. Björkling F, Frykman H, Godtfredsen SE, Kirk O (1992) Tetrahedron 48:4587–4592
13. Carter P, Wells JA (1988) Nature 332:564–568
14. Stoute VA, Winnik MA, Csizmiadia IG (1974) J Am Chem Soc 96:6388–6393
15. Okuno Y (1997) Chem Eur J 3:212–218
16. Cardenas R, Cetina R, Lagunez-Otero J, Reyes L (1997) J Phys Chem A 101:192–200
17. Cardenas R, Cetina R, Lagunez-Otero J, Reyes L (2000) J Mol Struct (THEOCHEM) 497:211–225
18. Hawthorne MF, Emmons WD, McCallum KS (1958) J Am Chem Soc 80:6393–6398
19. Carlqvist P, Eklund R, Brinck T (2001) J Org Chem 66:1193–1199
20. Hu C-H, Brinck T, Hult K (1998) Int J Quantum Chem 69:89–103
21. Morris GM, Goodsell DS, Halliday RS, Huey R, Hart WE, Belew RK, Olson AJ (1998) J Comput Chem 19:1639–1662
22. Guex N, Peitsch MC (1997) Electrophoresis 18:2714–2723
23. Weiner SJ, Kollman PA, Case DA, Singh UC, Ghio C, Alagona G, Profeta SJ, Weiner P (1984) J Am Chem Soc 106:765–784
24. Besler BH, Merz KM, Kollman PA (1990) J Comput Chem 11:431–439
25. Åqvist J, Medina C, Samuelsson J (1994) Protein Eng 7:385–391
26. Marelius J, Hanssson T, Åqvist J (1998) Int J Quantum Chem 69:77–88
27. Kollman PA (1993) Chem Rev 93:2395–2417
28. van Gunsteren WF, Berendsen HJC (1987) Groningen molecular simulation (GROMOS) library manual. Biomos, Groningen, The Netherlands
29. Marelius J, Kolmodin K, Feierberg I, Åqvist J (1998) J Mol Graph Model 16:213–225
30. Åqvist J, van Gunsteren WF, Leijonmarck M, Tapia O (1985) J Mol Biol 183:461–477
31. Becke AD (1993) J Chem Phys 98:5648–5652
32. Lee C, Yang W, Parr RG (1988) Phys Rev B 37:785–789
33. Martin JML, EL-Yazal J, Francois J-P (1995) Mol Phys 86:1437–1450
34. Bauschlicher Jr CW, Partridge H (1995) Chem Phys Lett 240:533–540
35. Frisch MJ, Trucks GW, Schlegel HB Scuseria GE, Robb MA, Cheeseman JR, Zakrzewski VG, Montgomery JA, Stratmann E, Burant JC, Dapprich S, Millam JM., Daniels AD, Kudin KN, Strain MC, Farkas O, Tomasi J, Barone V, Cossi M, Cammi R, Mennucci B, Pomelli C, Adamo C, Clifford S, Ochterski J, Petersson GA, Ayala PY, Cui Q, Morokuma K, Malick DK, Rabuck AD, Raghavachari K, Foresman JB, Cioslowski J, Ortiz JV, Baboul AG, Stefanov BB, Liu G, Liashenko A, Piskorz P, Komaromi I, Gomperts R, Martin RL, Fox DJ, Keith T, Al-Laham MA, Peng CY, Nanayakkara A, Gonzalez C, Challacombe M, Gill PMW, Johnson B, Chen W, Wong MW, Andres JL, Head-Gordon M, Replogle ES, Pople JA (1998) Gaussian 98, Rev A7. Gaussian, Pittsburgh Pa.